UNITED STATES DEPARTMENT OF THE INTERIOR
GEOLOGICAL SURVEY

Evolution of the Red Mountain alunite deposit, Lake City, Colorado

by

Dana J. Bove[1]
Robert O. Rye[1]
Ken Hon[2]

U.S. Geological Survey

Open-File Report 90-0235

1990

[1]Denver, CO 80225
[2]Hawaiian Volcano Observatory, Hawaii National Park, HI 96718

Contents

This report is a reformatted and expanded version of a talk presented at the annual meeting of the Geological Society of America in Denver, Colorado, November 3, 1988. (Bove et al., 1988). It is being released at this time because of obvious implications of this type of alunite occurrence for exploration of magmatic hydrothermal systems.

INTRODUCTION

Red Mountain, near Lake City, Colorado, is the site of one of the largest replacement alunite deposits in the western United States (with about 70 million metric tons of alunite). Exploratory drilling in 1979 established that the deposit overlies a weakly mineralized, molybdenite porphyry-type system. The purpose of this investigation is to use detailed mineralogic, petrographic, and stable isotope studies to determine the origin of the alunite and its relationship to the porphyry system at depth. Larson and Taylor (1987) concluded from an oxygen isotope study of drill core that the alunite at Red Mountain was formed from a meteoric-water hydrothermal system typical of those observed on the fringes of porphyry deposits. In contrast, we will conclude that the alunite formed from a buoyant magmatic vapor plume which rose above the level of the meteoric water-dominated fringe of the porphyry hydrothermal system and that the sulfur isotope systematics of the successive stages of alunites probably reflect the decreasing oxidation state of the underlying magma(s).

FIGURE 1. *Map of the San Juan volcanic field showing the Lake City (LC) caldera nested within the older San Juan (SJ) and Uncompaghre (UN) calderas (S, Silverton caldera).*

Calc-alkaline ash-flow activity began at about 28 m.y. ago in the western San Juan volcanic field, southwestern Colorado (Lipman and others, 1973). These early ash flow eruptions were closely followed by the simultaneous eruptions of the San Juan and Uncompaghre calderas (Lipman and others, 1973; Lipman and others, 1976). The Lake City caldera, nested within the older San Juan and Uncompaghre caldera complex, represents the youngest major caldera within the western San Juan volcanic field (Lipman and others, 1973; Steven and Lipman, 1976).

FIGURE 2. *Generalized geologic map of the Lake City caldera showing Red Mountain on the eastern margin.*

The Lake City caldera formed 23.1 m.y. ago in response to the large-scale eruption of the Sunshine Peak tuff (Mehnert and others, 1973). Accumulations of related ash-flow material exceeded 300 km^3, the majority of which ponded within the caldera along with subsidence-related collapse breccias. The intracaldera Sunshine Peak tuff, a compositionally zoned ash-flow sheet, contains three intragradational phases; these include an early (lower member) high-silica rhyolite (76% SiO_2), a middle rhyolitic member (74% SiO_2), and a late (upper member) quartz trachyte (68% SiO_2) (Hon, 1987). Only the early high-silica rhyolite, which is the most voluminous of the three units, is preserved within the outflow sheet. Potassium-argon ages of the upper and middle members are 23.2 ± 1.2 Ma and 24.0 ± 1.2 Ma, respectively. Based on recent paleomagnetic studies (Reynolds and others, 1986), the duration of the Lake City caldera activity from ash-flow eruption to resurgent doming was less than 300,000 years.

FIGURE 3. *Simplified geologic map of the Red Mountain area.*

Red Mountain formed on the eastern margin of the 23.1 Ma Lake City caldera. Several texturally and temporally distinct high-potassium dacite intrusions cut earlier post-caldera collapse, high-potassium dacite lavas on Red Mountain. Potassium-argon dating (Mehnert and others, 1973, 1979) and geologic evidence (Bove, 1988, Bove and Hon, in press) indicate that emplacement of the lavas and intrusions on Red Mountain, as well as

alunite alteration, occurred contemporaneously with the eruptive cycle of the 23.1 Ma Lake City caldera.

The dacite lavas of Grassy Mountain, were erupted along the eastern ring fracture zone following caldera collapse. These rocks range from 63 to 66% SiO_2 and average 5.2% K_2O. The dacite lavas bracket resurgent doming of the caldera; the lavas to the south of Red Mountain pre-date caldera resurgence; whereas the lavas to the north of Red Mountain post-date resurgence. Although these lavas pre-and post date caldera resurgence, they are indistinguishable texturally, geochemically, and isotopically. Potassium-argon dating of the dacite lavas yielded an age of 23.4 ± 1.2 Ma (Mehnert and others, 1973).

The dacite lavas have been intruded by a series of temporally and texturally distinct high-potassium dacite porphyry intrusions collectively referred to as the Dacite of Red Mountain. Fresh rock analyses from these intrusions range from 63 to 65% SiO_2 with an average of 4.7% K_2O. All but the latest of the dacite intrusions have been alunitized. Alunite alteration, which is outlined by the dashed line, has been dated at about 23 Ma (Mehnert and others, 1979).

FIGURE 4. *Map view of hydrothermal alteration at Red Mountain. A-A' is line of cross section in Figure 5.*

A large zone of quartz-alunite altered rock (QA) grades outward into intermediate argillic alteration (I), farther outward into weak argillic alteration (W), and finally into what has been termed marginal alteration (M). The alunite alteration assemblage is characterized by the presence of alunite, quartz, and pyrite, with minor amounts of topaz, pyrophyllite, and gypsum. The argillic alteration assemblages are characterized by the presence of kaolinite, sericite, pyrite, and minor smectite. Both sanidine and plagioclase are completely altered in the intermediate assemblage, whereas sanidine is unaltered in the weak argillic assemblage. Marginal alteration is characterized by a light dusting of sericite and smectite, and the absence of pyrite.

FIGURE 5. *Cross section showing alteration at Red Mountain as extrapolated from drill logs (LC1-4) and surface mapping.*

Quartz-alunite alteration (QA) occurred in two large, nearly conical centers whose roots extend more than 820 ft beneath the surface. Within the quartz-alunite assemblage (QA), alunite generally makes up at least 30 volume percent of the rock. These zones of alunite-altered rock account for a minimum estimated resource of 70 million metric tons of alunite. Pyrite, which comprises an average of 5 volume percent of the rock in the quartz-alunite assemblage, is oxidized to hematite, jarosite, and limonite in upper levels of the quartz-alunite zone.

Alunitized rocks grade downward into zones of argillic and potassic alteration zones that are dominantly within dacite intrusions. In argillically altered rocks, kaolinite overprints earlier sericite ± pyrite. Kaolinite is the dominant clay in the argillic zone to a depth nearly 1,846 ft beneath the top of Red Mountain; however, sericite predominates below that level. From geologic inference we have been able to establish that the quartz-alunite alteration assemblage at Red Mountain is integrally related to the hydrothermal system that produced classic porphyry-style alteration at depth (Bove, 1988).

FIGURE 6a. *Distribution of molybdenite in drill hole LC-4.*

Weak porphyry-type mineralization is found throughout drill-hole LC-4 (total depth 2,777 ft), with molybdenite present mostly along hairline fractures in association with late pyrite ± sericite ± quartz. The highest molybdenite concentrations (150 to 1150 ppm) occur over a roughly 1,500 ft interval and are generally coincident with the zone of potassic alteration (fig. 6a). Elevated concentrations of Cu, Pb, and Zn were also detected in the same drill hole, but only rare, finely disseminated sphalerite and chalcopyrite could be identified.

FIGURE 6b. *F/Cl intercept versus F intercept plots of biotites from Red Mountain (filled circles), Henderson (X), and Santa Rita (+). Data from Henderson and Santa Rita from Munoz (1984).*

Electron microprobe analyses of hydrothermal sericite and biotite from several samples from drill hole LC-4, focusing primarily on F and Cl content of the micas, were used to compare the Red Mountain hydrothermal system to the porphyry systems characterized by Munoz (1984). Halogen intercept values[1] of the micas were calculated from microprobe analyses to determine the relative enrichment of F and Cl in the micas and to correct for the opposing effects of Mg/Fe ratio on F=OH and Cl=OH exchange.

Figure 6b is a plot comparing F/Cl versus F intercept values of biotites from Red Mountain to those from the Henderson Mo-porphyry deposit and the Santa Rita porphyry Cu deposit. The Red Mountain biotites fall in an area that lies between the Henderson and Santa Rita biotites. As indicated in figure 6b relic magmatic biotites have undergone hydrothermal F enrichment (corresponding to lower IV(F) values), although TiO_2 and SiO_2 contents are somewhat higher than the hydrothermal biotites, more closely resembling magmatic values. Sericites from Red Mountain have F intercept values that cluster near the lowest IV(F) values (IV(F) range: 0.98-1.07) of the hydrothermal and relic magmatic biotites. Because the lower IV(F) values for sericite correspond to higher degrees of F enrichment, these data suggest that the earlier formed secondary biotite exchanged with later sericite-forming fluids.

The occurrence of anomalous molybdenum coupled with the overall pattern of alteration, presence of multiple intrusions, and high F intercept values of sericite and secondary biotite, suggest the presence of a relatively high F, low silica Mo-porphyry system at depth. Plots comparing F versus F/Cl intercepts (fig 6b) illustrate that micas in the Red Mountain porphyry system fall in a region between a quartz monzonite-granodiorite Cu-porphyry system such as Santa Rita, and a high-silica granite Mo-porphyry system as exemplified by the Henderson deposit. Unfortunately, chemical analyses of micas from quartz monzonite-granodiorite Mo-porphyry systems (Soregaroli and Sutherland Brown, 1976; Theodore, 1982) were not available at the time of this writing for comparison to those from Red Mountain.

Four major stages of alunitization have been differentiated by detailed petrographic and SEM studies. Separation of these individual stages was critical for the stable isotope study.

FIGURE 7a. *Photograph of stage 1 alunitized dacite porphyry intrusion.*
FIGURE 7b. *Photomicrograph showing stage 1 alunite (very fine white material), which has replaced feldspar phenocrysts. The groundmass consists of very fine-grained quartz, minor alunite, and finely disseminated pyrite. (Field of view 1 cm).*

Stage 1, which marks the earliest episode of alunite alteration, is characterized by the concurrent replacement of feldspar phenocrysts by very fine-grained alunite ± minor quartz and groundmass alteration to a dense, gray mixture of quartz, lesser amounts of alunite, and finely disseminated pyrite.

Prior to stage 2 there was a change in the fluid chemistry of the system, which resulted in partial dissolution of stage 1 alunite. Quartz and pyrite remained stable during this dissolution event.

---

[1]IV(F) for biotite= $1.52\ X_{Mg} + 0.42\ X_{An} + 0.20\ X_{Sid} - \log (X_F/X_{OH})$
IV(F) for sericite= $1.52\ X_{Mg} + 0.42\ X_{Fe} - 0.11\ X_{Al} - \log (X_F/X_{OH})$ IV(F/Cl) for biotite= $3.45\ X_{Mg} + 0.42\ X_{An} + 0.20\ X_{sid} - \log (X_F/X_{Cl}) + 5.01$ where X_{An} and X_{Sid} are mole fraction of annite and sideropyllite components (Munoz, 1984)

FIGURE 8a. *Photomicrograph of stage 2 lath-shaped alunite crystals that formed in microscopic void space created by the dissolution of stage 1 alunite. Field of view 1 cm.*
FIGURE 8b. *SEM micrograph depicting stage 2 alunite (A) with crystals terminating into microscopic void space created by dissolution. Alunite has grown from stage 1 quartz and alunite.*
FIGURE 8c. *SEM view of early (E) and late (L) topaz crystals. Early topaz is contemporaneous with stage 2 alunite, whereas late topaz has grown on top of stage 2 alunite. (A, alunite, Q, quartz).*

Stage 2 alunite is characterized by multiple generations of void- and micro-fracture-filling alunite and lesser amounts of quartz that precipitated in an alternating sequence. In addition, finely disseminated pyrite and two stages of topaz (fig. 8c) formed during this period. During stage 2, quartz-alunite-saturated fluids moved along networks of microfractures, flooded the groundmass, and infiltrated previously altered and variably dissolved phenocryst sites via the fracture network. Stage 2 alunite typically nucleated from webs of undissolved pre-stage 2 quartz or grew from patches of undissolved stage 1 alunite.

FIGURE 9. *Stage 3 alunite veins.*

Stage 3 is characterized by very fine-grained, white, fracture-filling alunite ± minor quartz. These veins generally average several mm in width although a few veins up to 3 to 5 cm have been observed. Vein margins are extremely sharp to highly diffuse, varying with increasing replacement of pre-stage 3 alunite-altered wallrock. Although present throughout the extent of the quartz-alunite zone, stage 3 veins are anomalously concentrated in areas affected by extreme hydrothermal brecciation.

FIGURE 10. *Vein of stage 4 alunite.*

Veins and veinlets of flesh-colored, translucent alunite comprise stage 4. By far the rarest of the stages, stage 4 veins have been observed in only one of three drill-holes that penetrated quartz-alunite altered rock. Veinlets contain fan-shaped aggregates of euhedral lath-shaped alunite that have bladed or feathery terminations. Vein widths are highly variable never exceeding 1 cm, and margins are sharp. Stage 4 veins, which mark the latest episode of alunite mineralization, commonly cut stage 3 veinlets.

FIGURE 11. *Sulfur isotope data of various stages of alunite and coexisting pyrite and pyrite in underlying sericite and potassic alteration zones.*

The total range of $\delta^{34}S$ values for alunite is about -3 to 27‰. However, each stage of alunite has distinct $\delta^{34}S$ values values: stage 1 (8.4 to 10.7‰), stage 2 (17.6 to 27.2‰), stages 3 and 4 (-3.9 to 0.1‰). The range of $\delta^{34}S$ of pyrite is much less from about -8.1 to 0 ‰. However, each stage of pyrite also has distinct $\delta^{34}S$ values and the $\delta^{34}S$ values for pyrite in stages 1 and 2 are distinctly lower than those for pyrite associated with the sericitic alteration. It is important to note that the $\delta^{34}S$ values of alunite in stages 3 and 4, which do not have associated pyrite, are generally larger than those observed for pyrite in stages 1 and 2 and are close to those of pyrite associated with the underlying sericitic alteration.

FIGURE 12. *Interpretation of sulfur isotope data in terms of assumed constant $\delta^{34}S$ of hydrothermal solutions.*

The interpretation of sulfur isotope data requires knowledge of the $\delta^{34}S$ of the bulk sulfur in the hydrothermal system as well as information on temperature and oxidation state of hydrothermal fluids (Ohmoto 1972). We do not have independent data on the $\delta^{34}S$ of the bulk sulfur or the H_2S/SO_4 of the system. If we make the reasonable assumption that the $\delta^{34}S$ of the total sulfur in the system was constant with a value near 0‰ --the value often typical of the deep sulfides in igneous environments-- the $\delta^{34}S$ data can be interpreted in terms of changing sulfur speciation in the fluids. Temperatures for stage 1 and 2 alunites

can be calculated from the $\delta^{34}S$ data on coexisting alunite and pyrite using the curves of Ohmoto and Rye (1979). Calculated temperatures based on these fractionations are nearly 400°C for stage 1 and about 200°C for the isotopically heaviest alunite in stage 2. When the $\delta^{34}S$ values of pyrite and alunite are converted to values for hydrothermal H_2S and SO_4, respectively, the sulfur isotope fractionation between H_2S and SO_4 in the fluid can be shown to have increased from stage 1 to 2. If the $\delta^{34}S$ of the bulk sulfur was 0‰, the H_2S/SO_4 of the fluid increased from about 1 for stage 1 to about 6 for the heaviest alunite in stage 2.

The large $\delta^{34}S$ values of the alunite in stages 1 and 2 were derived from equilibration of hydrothermal sulfate with isotopically lighter H_2S in the hydrothermal system. This sulfate most likely formed from the disproportionation of SO_2 (Stoffregen, 1988; Rye et al., 1988) which must have been derived from an underlying magma. Pyrite does not occur in stages 3 and 4, but the low $\delta^{34}S$ values of the alunites almost require that their sulfate was derived from the oxidation of H_2S, and the $\delta^{34}S$ values of the alunites probably reflect the $\delta^{34}S$ of this H_2S. Thus, the $\delta^{34}S$ of H_2S in the system increased from about -8 to 0‰ from stage 1 to 4. During the last stage of alunite formation the H_2S obtained the same value as that of the total sulfur in the system. This suggests a large H_2S/SO_4 ratio for the late fluids and implies that the sulfur isotope systematics reflect a decrease in the f_{O2} as the temperature of the system dropped. The simplest interpretation is to relate this decrease in f_{O2} of the fluids to a decrease in the f_{O2} of an evolving magma or to increasing equilibration of magmatic fluids with reduced country rocks. Figures 13a and b show how the changes in the H_2S/SO_4 of the alunite fluids may have related to the possible change in oxidation state of parent magmas.

FIGURE 13a. *fO_2-T diagram for sulfide-saturated equilibria portraying interpreted conditions in pyrrhotite-bearing magmas for various magmas (adapted from Whitney, 1988): Julcani vitrophyres (J), El Chichon ash (EC), Fish Canyon Tuff, (FC) St. Helens ash (SH) and Bishop Tuff (B). Initial conditions for Red Mountain (RM) magmas consistent with sulfur isotope data are indicated by arrow.*

Unoxidized igneous rocks at Red Mountain are not available for study. However, from textural evidence the dacite lavas at Red Mountain (RM) originally contained pyrrhotite and magnetite and recent studies (R.O. Rye, unpublished data) have indicated that apatite in these rocks has high concentrations of sulfate. The initial magma had temperatures of 900°C (Bove, 1988) and it is reasonable to assume that the f_{O2} was within the $SO_4^=$ dominant field. The trajectory on Figure 13a reflects the temperature decrease and the decrease in the oxidation state of the later magma(s) that would account for the increase in H_2S/SO_4 of the various fluid stages.

FIGURE 13b. *Predicted concentration of sulfur species in 250°C hydrothermal solutions derived from 900°C magmas as a function of initial oxygen fugacity of the magma (Whitney, 1988) showing values indicated by stage 1,2 and 3-4 alunite sulfur isotope data.*

The three shaded areas show the oxidation state of parent magmas required by the H_2S/SO_4 of the fluids as indicated by the sulfur isotope data for the various stages of alunite. This model is based on the assumption that the hydrothermal system was in isotopic equilibrium and was closed to isotopic and chemical exchange with wall rocks. These assumptions are probably not unrealistic for a magmatic vapor plume that operated in hydrothermally brecciated rock. This diagram assumes constant temperature of the source magmas whereas the later stage fluids probably evolved from cooler magmas so Figure 13b is really schematic for the Red Mountain system. Also the depositional temperature of stage 1 alunites was probably greater than 250°C. The point here, however, is that the sulfur isotope systematics can very easily be explained qualitatively as the result of a decrease in the f_{O2} of the magma(s). Such a decrease may be due to the loss of SO_2 from the magma(s) (Whitney, 1988). Below we will consider why the suggested f_{O2} decrease

of the fluid was probably due to changes in the magma and not to mixing of the hydrothermal fluids with meteoric water or reaction with wall rocks.

FIGURE 14. *$\delta^{34}S$ and $\delta^{18}O_{SO4}$ values of stage 1-4 alunite.*

Stage 1 shows a narrow range of $\delta^{18}O$ and $\delta^{34}S$ values and stage 2 alunites show a good correlation between these values. The narrow range of values for stage 1 alunite reflects deposition from fluids of uniform temperature and composition. Temperature of deposition can be calculated to have been about 400°C from the alunite-pyrite fractionations. The alunite-pyrite fractionations indicate a temperature of about 200°C for the isotopically heaviest stage 2 alunites. The previous diagram indicated that the isotope systematics of successive stages of alunite can be explained as a result of decrease in the oxidation state of the underlying magma. The correlation between $\delta^{18}O$ and $\delta^{34}S$ values may reflect a continual decrease in the H_2S/SO_4 of the fluids derived from a magma that underwent continual decrease in oxidation state due to the loss of SO_2. However, Stage 1 alunite is partially dissolved and the correlation of $\delta^{18}O$ and $\delta^{34}S$ values for stage 2 may reflect the mixing of dissolved stage 1 sulfate and sulfate in the stage 2 fluids. The $\delta^{18}O$ of the water and the $\delta^{34}S$ of total sulfur in the fluids, calculated using the temperature information shown on Figure 14, were buffered at about 4 and 0 ‰, respectively, during stages 1 and 2. The temperatures of stage 3 and 4 alunite deposition are unknown. The sulfur isotope data indicate that stage 3 and 4 alunites were derived from the oxidation of H_2S. This oxidation probably involved atmospheric oxygen which has a $\delta^{18}O$ of 23 ‰. The intermediate $\delta^{18}O_{SO4}$ values of the late alunites indicates that the oxygen in their sulfate probably also equilibrated with the isotopically buffered water in the hydrothermal fluids. The fact that this equilibration did not also affect the sulfur isotope composition of the alunite probably reflect the slower exchange rates for sulfur versus oxygen isotopes in hydrothermal systems (cf., Ohmoto and Lasaga, 1982; Chiba, 1985). This inference of oxygen isotope equilibration with hydrothermal fluids is supported by the δD data discussed below.

FIGURE 15. *δD and $\delta^{18}O$ data on alunite, kaolinite and sericite.*

δD values of alunite have a narrow range averaging about -75 ‰ and a wide range of $\delta^{18}O$ values from about 8 to 15 ‰. These alunite compositions cluster in a field entirely different from the kaolinites and sericites in Figure 15. The calculated δD of fluids in equilibrium with stage 1 and 2 alunites average about -70 and $\delta^{18}O$ values average about 4 ‰. The values were calculated using the experimental alunite-water hydrogen and oxygen isotope fractionation factors of Stoffregen et al. (1990). The calculated δD values for the kaolinite and sericite fluids average about -120 ‰ while the $\delta^{18}O_{H2O}$ values were between about 0 to -10 ‰. Since all alunites have a limited range of δD values it is likely that all alunite fluids were predominantly magmatic and not mixtures of magmatic and meteoric water and were unlike the meteoric water dominated sericite and kaolinite fluids. The next figures will show how we believe the magmatic and meteoric systems were related.

FIGURE 16a *Model for stage 1 and 2 hydrothermal systems showing isotherms, alteration zones including central zones of h hydrothermal brecciation and meteoric and magmatic recharge areas for hydrothermal system.*

FIGURE 16b *Model for stage 3 and 4 hydrothermal systems showing isotherms, alteration zones including central zones of hydrothermal brecciation and meteoric and magmatic recharge areas for the hydrothermal system.*

Detailed mineralogic, petrographic, and stable isotope studies provide critical constraints for the following model which outlines the evolution of the Red Mountain hydrothermal system. Hydrogen, oxygen, and sulfur stable isotope data constrain the origin of the alunite and the source of the fluids and sulfur. Each stage of alunite has a distinctly different isotopic composition as do the different generations of pyrite. These data suggest that stage 1 alunite formed from sulfate derived from a magmatic source at

temperatures above 350°C and stage 2 alunite formed from the same sulfur sources at about 200°C. In contrast, late stage 3 and 4 alunite was derived from the surficial oxidation of H_2S.

At depth, classic porphyry-style alteration formed synchronously with the emplacment of one or more dacite porphyry intrusions. Porphyry-style alteration is represented by the deep potassic alteration assemblage, which is superimposed by sericitic alteration. The sericite assemblage was formed by a meteoric water-dominated system that was recharged on the flanks of the resurgent dome of the Lake City caldera. Alunite, which grades outward into an argillic alteration assemblage , represents the upper levels of the porphyry hydrothermal system. Stage 1 and 2 alunite formed from a buoyant magmatic vapor plume that was derived from a fairly oxidizing magma. This plume rose along conduits of fractures and hydrothermally brecciated rock above the level of the meteoric water, porphyry alteration envelope. Stage 1 and 2 alunite was derived from the disproportionation of SO_2 that was derived from the dacite magma. The lateral argillic alteration assemblage reflects the mixing of the alunite-forming fluids with meteoric-dominant water. Stage 3 and 4 alunite formed similarly to alunite of stages 1 and 2. however, the magmatic vapor plume was probably much smaller, and the source magma was more reduced. These late-stage alunites have limited distribution and probably formed from the oxidation of H_2S by atmospheric oxygen entrained in the upper part of the waning hydrothermal system.

These diagrams are highly idealized. Our ability to draw qualitative models is limited by the fact that we have only one deep drill hole and we can not study the detailed paragenetic relationships between the alunite and underlying porphyry system. However, the flux of the magmatic plume was probably episodic. We also do not know if the magmatic plume exsolved from a single magma or a series of related magmas. The most important point here is that the alunites formed almost entirely from magmatic fluids which reached higher levels than the meteoric water hydrothermal system and detailed study of these alunites can be used to recognize the magmatic system and to trace some of its physical chemical evolution.

REFERENCES

Bove, D J., 1988, Evolution of the Red Mountain alunite deposit, Lake City caldera, San Juan Mountains, Colorado, 1988, University of Colorado, Boulder, unpublished masters thesis, 179 p.

Bove, D. J., and Hon, Ken, in press, Geologic and alteration maps and drill core logs of the Red Mountain alunite deposit near Lake City, Hinsdale County, Colorado: U.S. Geological Survey I-Series Map 88-358.

Bove, D.J., Rye, R.O., and Hon, Ken., 1988, Evolution of the Red Mountain alunite deposits, Lake City, Colo [abst.]: Geological Society of America Abstracts with Programs, v. 20, p. A353.

Chiba, H., Kusakabe, M., Hirano, S., Matsuo, S., and Somiya, S, 1981, Oxygen isotope fractionation factors between anhydrite and water from 100 to 500°C: Earth Planet. Science Letters, v. 53, p. 55-62.

Hon, Ken, 1987, Geologic and petrologic evolution of the Lake City caldera, San Juan Mountains, Colorado: University of Colorado, Boulder, unpublished PhD. dissertation, 244 p.

Larson P. B. and Taylor, H.P., Jr., 1987, Solfataric alteration in the San Juan Mountains, Colorado; oxygen isotope variations in a boiling hydrothermal environment: Economic Geology v. 82, p. 1019-1036.

Lipman, P. W., Fisher, F.S.., Mehnert, H.H., Naeser, C.W., Luedke, R. G., Steven, T. A., 1976, Multiple ages of mid-Tertiary mineralization and alteration in the western San Juan Mountains, Colorado: Economic Geology, v. 71, p. 571-588.

Lipman, P. W., Steven, T. A., Luedke, R. G., and Burbank, W.S., 1973, Revised volcanic history of the San Juan, Uncompahgre, Silverton, and Lake city calderas

in the western San Juan Mountains, Colorado: U.S. Geological Survey Journal of Research, v. 1, p. 627-642.
Mehnert, H. H., Lipman, P. W., and Steven, T. A., 1973, Age of the Lake City caldera and related Sunshine Peak Tuff, western San Juan Mountains, Colorado: Isochron/West, no. 6, p. 31-33.
Mehnert, H. H., Slack, J. F., and Cebula, G. T., 1979, K-Ar age of alunite alteration at Red Mountain, Lake City area, western San Juan Mountains, Colorado: U.S. Geological Survey Open-File Report 79-1642, 8 p.
Munoz, J.L., 1984, F-OH and Cl-OH exchange in Micas with applications to hydrothermal ore deposits, in Bailey, S.W., ed., Reviews in mineralogy, micas, vol. 13, Mineralogical Society of America, p. 461-491.
Ohmoto, H., 1972, Systematics of sulfur and carbon isotopes in hydrothermal ore deposits: Economic Geology., v. 67, p. 551-579.
Ohmoto, H. and Rye, R.O., 1979, Isotopes of sulfur and carbon,in Barnes, H.L. (ed.), Geochemistry of hydrothermal ore deposits, Holt Rinehart, and Winston, New York, p. 509-567.
Ohmoto, H. and Lasaga, A.C., 1982, Kinetics of reactions between aqueous sulfates and sulfides in hydrothermal systems: Geochim. Cosmochim Acta, v. 46, p. 1727-1746.
Reynolds, R.L. Hudson, M.R., and Hon, Ken, 1986, Paleomagnetic evidence regarding the timing of collapse and resurgence of the Lake City caldera, San Juan Mountains, Colorado: Journal of Geophysical Research, vol. 91, p. 9599-9613.
Rye, R.O. Bethke, P.M., and Wasserman, M.D., 1989, Diverse origins of alunite and acid-sulfate alteration: stable isotope systematics: U.S. Geological Survey Open-File Report 89-5, 33 p.
Soregaroli, A.E., and Sutherland Brown, A., 1976, Characteristics of Canadian Cordilleran molybdenum deposits, in Sutherland Brown, A., ed., Porphyry deposits of the Canadian Cordillera, Ney Volume, p. 432-443.
Steven, T.A., and Lipman, P.W., 1976, Calderas of the San Juan volcanic field, southwestern Colorado: U.S. Geological Survey Professional Paper 958., 35 p.
Stoffregen, R.E., 1988, Genesis of acid-sulfate alteration and Au-Cu-Ag mineralization at Summitville, Colorado: Economic. Geology, v. 82, p. 1575-1591.
Stoffregen, R.E., Rye, R.O., and Wasserman, M.D., 1989, Experimental determination of 18O (sulfate-site) and D fractionations between alunite and water at 250 to 450°C [abs.]: Geological Society of America Abstracts with Programs v. 21, p. A155.
Theodore, T.G., 1982, Preliminary model outline for fluorine-deficient porphyry molybdenum deposits, in Erickson, R.L., ed., Characteristics of mineral deposit occurrences, U.S. Geological Survey Open-File Report 82-795, p. 37-42.
Whitney, J.A., 1988, Composition and activity of sulfurous species in quenched magmatic gases associated with pyrrhotite-bearing silicic systems: Economic Geology v. 83, p. 86-92.

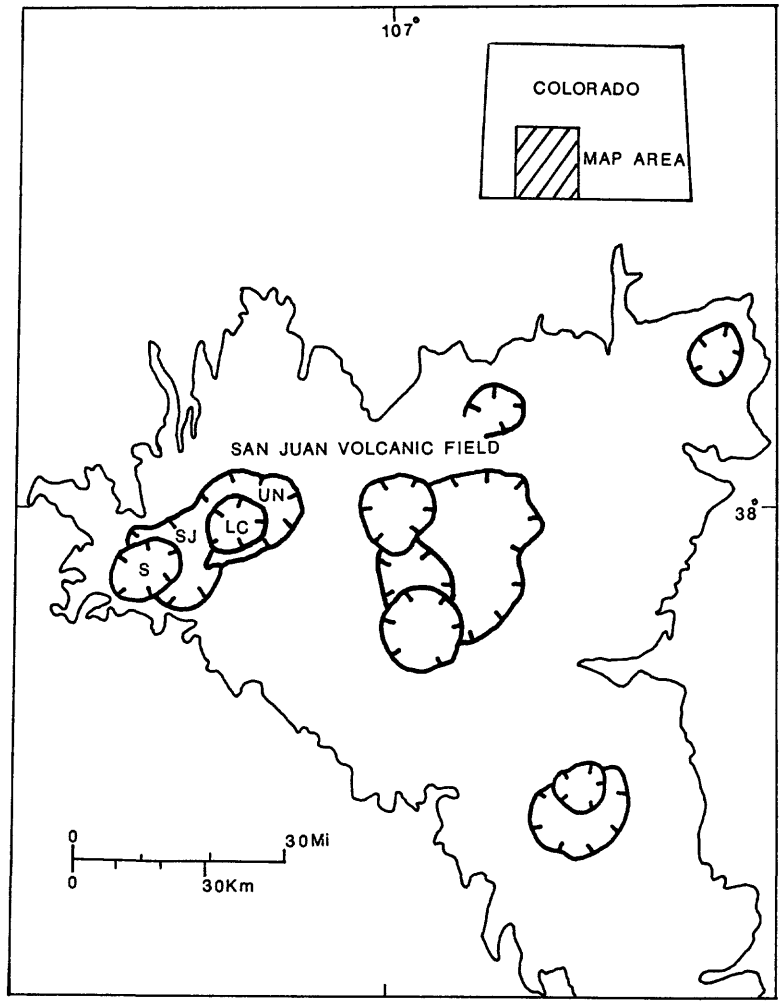
107°
COLORADO
MAP AREA
SAN JUAN VOLCANIC FIELD
UN
LC
SJ
S
38°
0
30Mi
0
30Km

Figure 1.

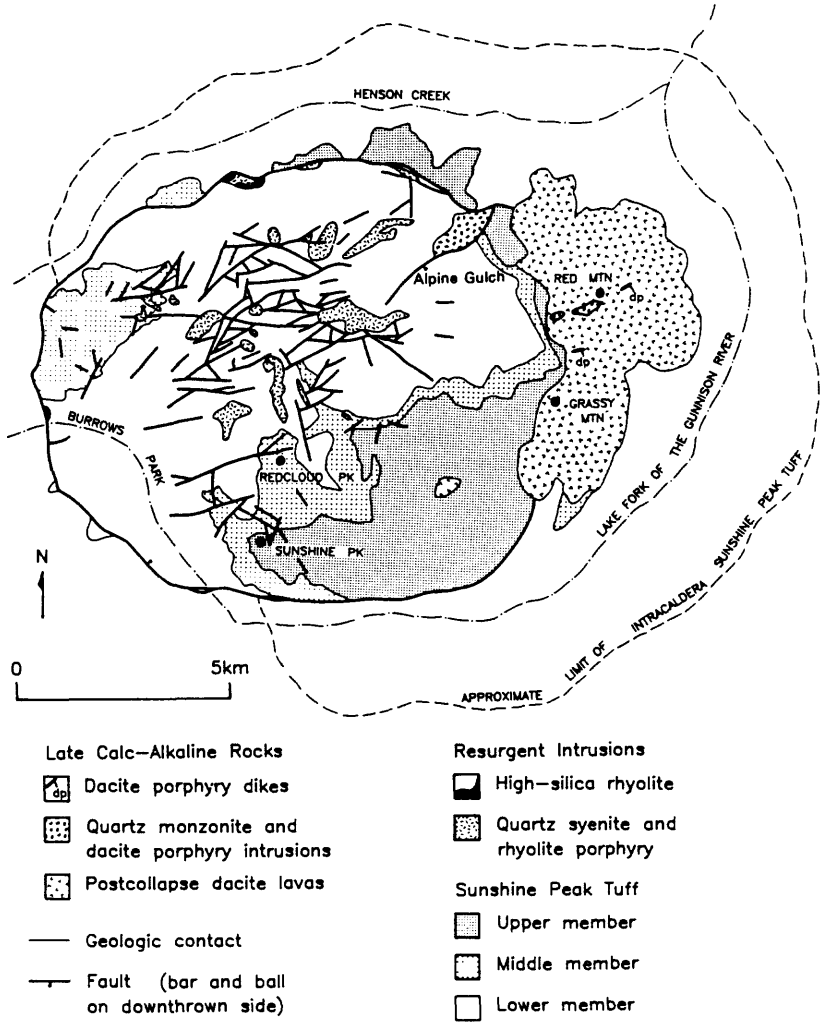
HENSON CREEK
Alpine Gulch
RED MTN
dp
dp
GRASSY MTN
BURROWS PARK
REDCLOUD PK
SUNSHINE PK
LAKE FORK OF THE GUNNISON RIVER
SUNSHINE PEAK TUFF
INTRACALDERA
LIMIT OF
APPROXIMATE
N
0
5km
Late Calc–Alkaline Rocks
dp Dacite porphyry dikes
Quartz monzonite and dacite porphyry intrusions
Postcollapse dacite lavas
Geologic contact
Fault (bar and ball on downthrown side)
Resurgent Intrusions
High–silica rhyolite
Quartz syenite and rhyolite porphyry
Sunshine Peak Tuff
Upper member
Middle member
Lower member

Figure 2.

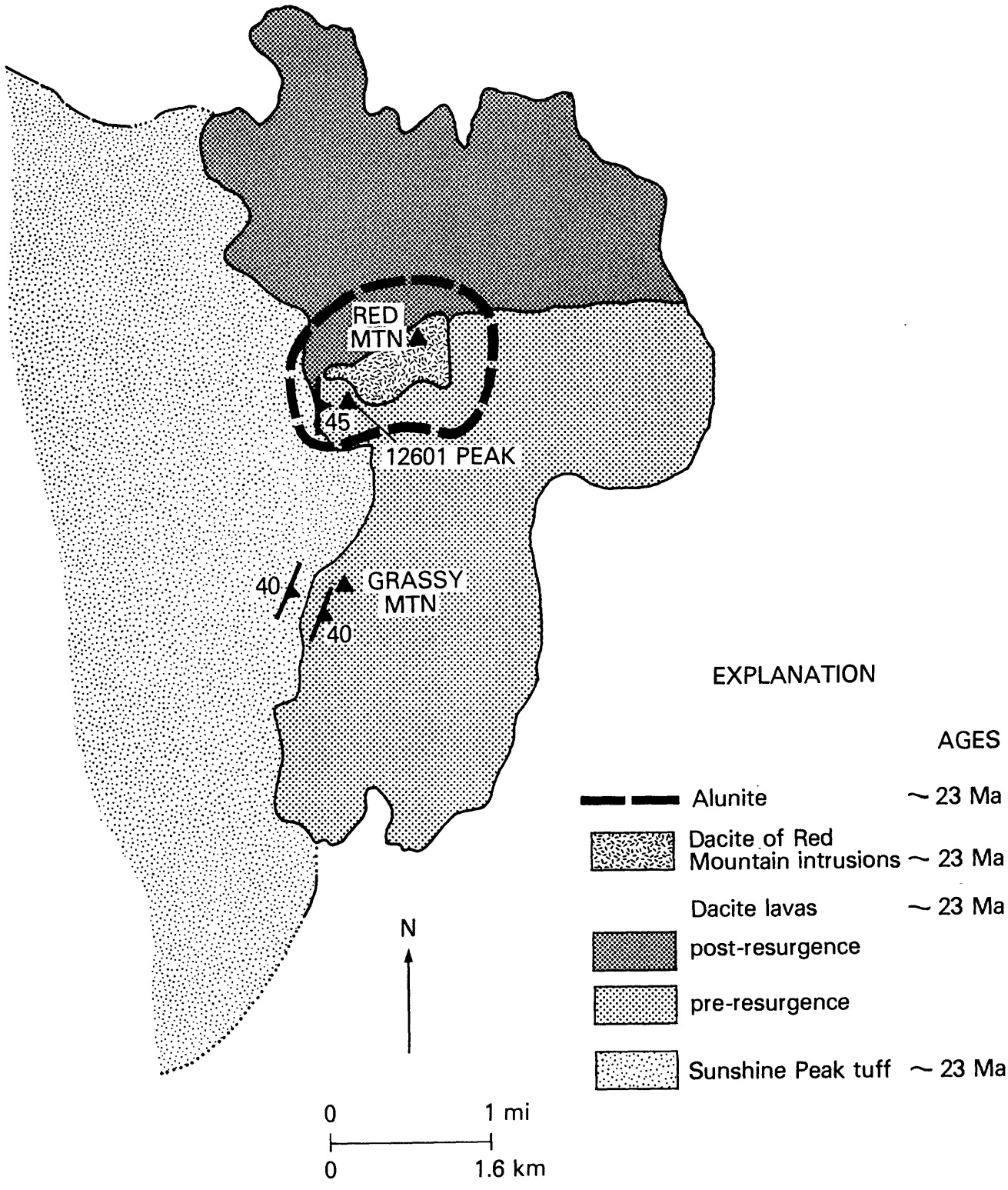
SIMPLIFIED GEOLOGY OF RED MOUNTAIN AREA
RED MTN
45
12601 PEAK
40
GRASSY MTN
40
N
0
1 mi
0
1.6 km
EXPLANATION
AGES
Alunite
~ 23 Ma
Dacite of Red Mountain intrusions
~ 23 Ma
Dacite lavas
~ 23 Ma
post-resurgence
pre-resurgence
Sunshine Peak tuff
~ 23 Ma

Figure 3.

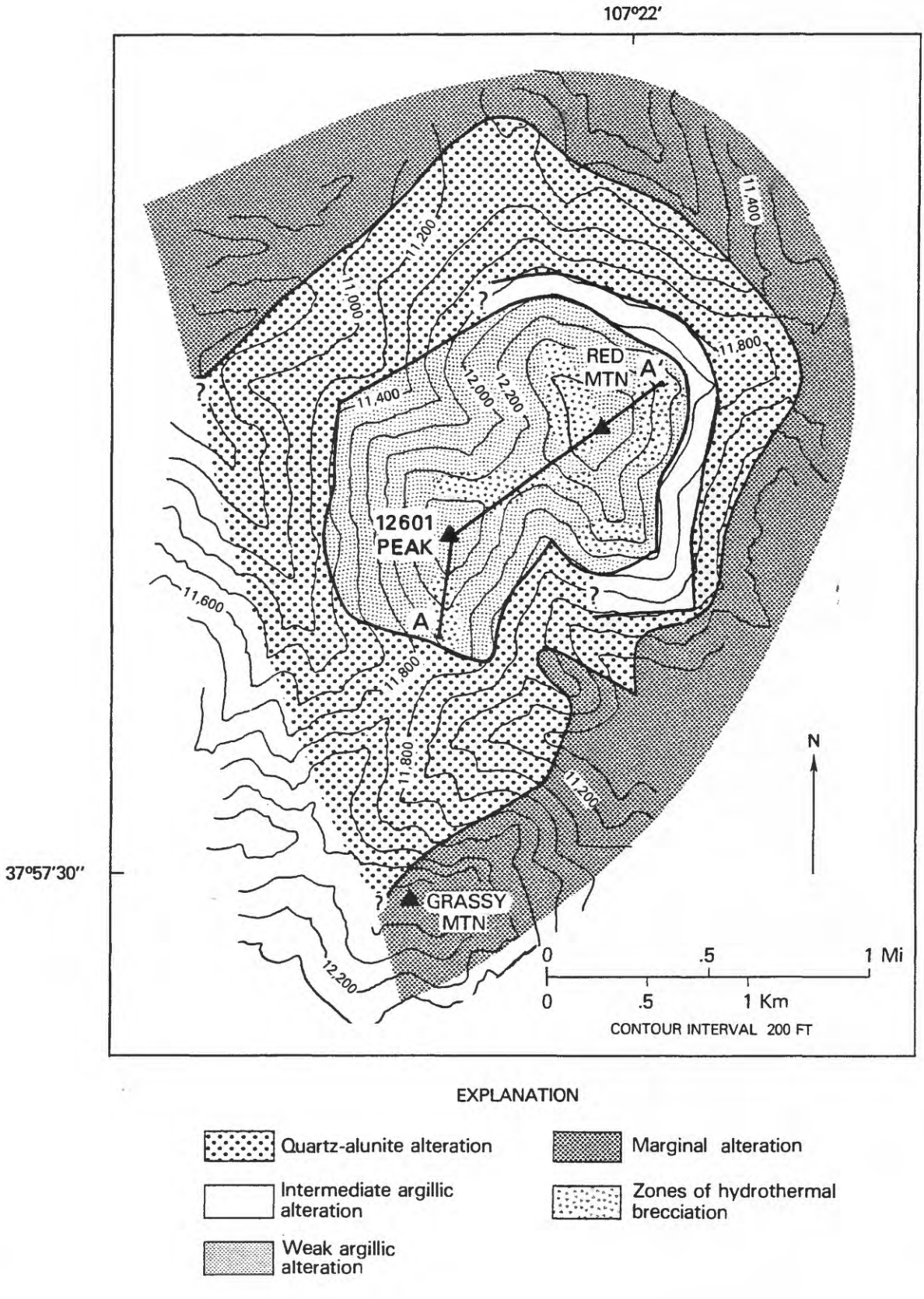
107°22'
37°57'30"
11,400
11,200
11,000
11,800
12,000
12,200
11,600
RED MTN
A'
A
12601 PEAK
GRASSY MTN
N
0 .5 1 Mi
0 .5 1 Km
CONTOUR INTERVAL 200 FT
EXPLANATION
Quartz-alunite alteration
Marginal alteration
Intermediate argillic alteration
Zones of hydrothermal brecciation
Weak argillic alteration

Figure 4.

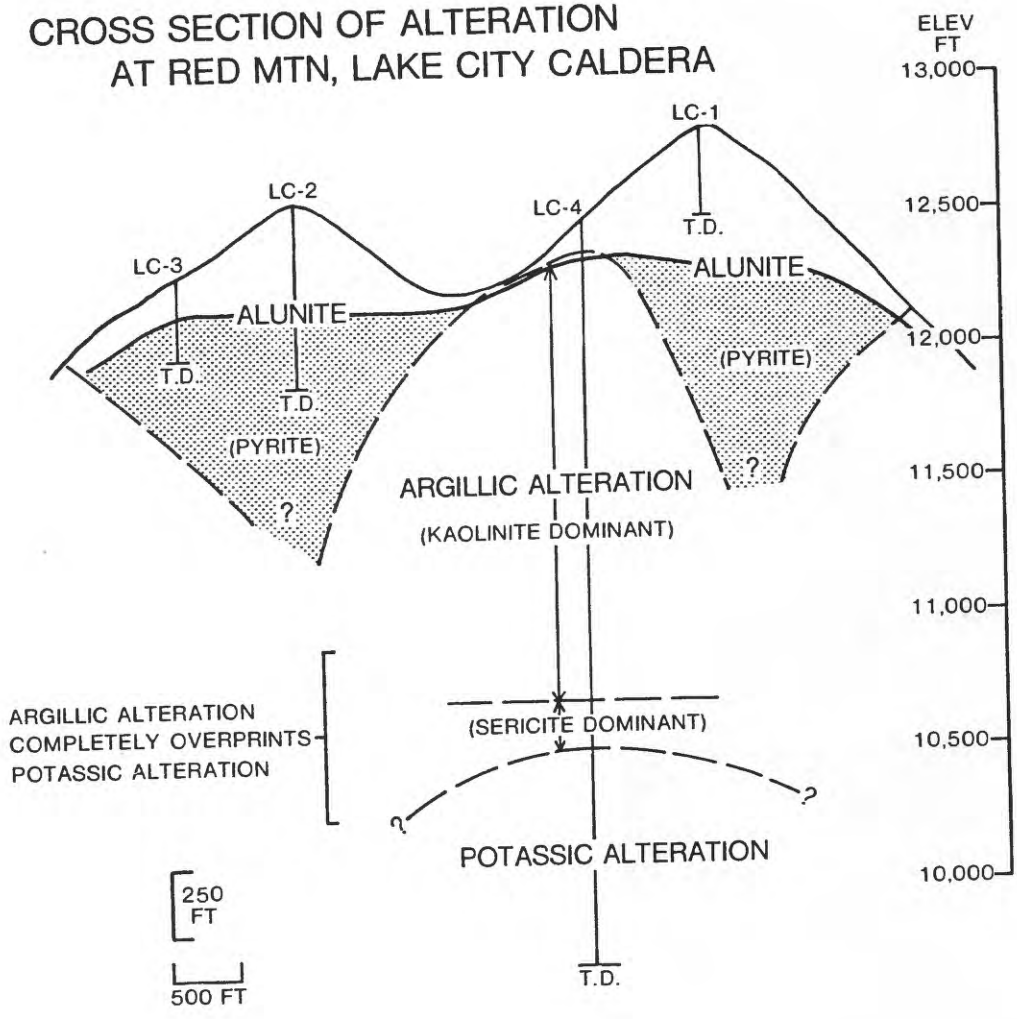
CROSS SECTION OF ALTERATION
AT RED MTN, LAKE CITY CALDERA
ELEV
FT
13,000
12,500
12,000
11,500
11,000
10,500
10,000
LC-1
LC-2
LC-3
LC-4
T.D.
T.D.
T.D.
T.D.
ALUNITE
ALUNITE
(PYRITE)
(PYRITE)
?
?
ARGILLIC ALTERATION
(KAOLINITE DOMINANT)
(SERICITE DOMINANT)
ARGILLIC ALTERATION
COMPLETELY OVERPRINTS
POTASSIC ALTERATION
POTASSIC ALTERATION
250
FT
500 FT

Figure 5.

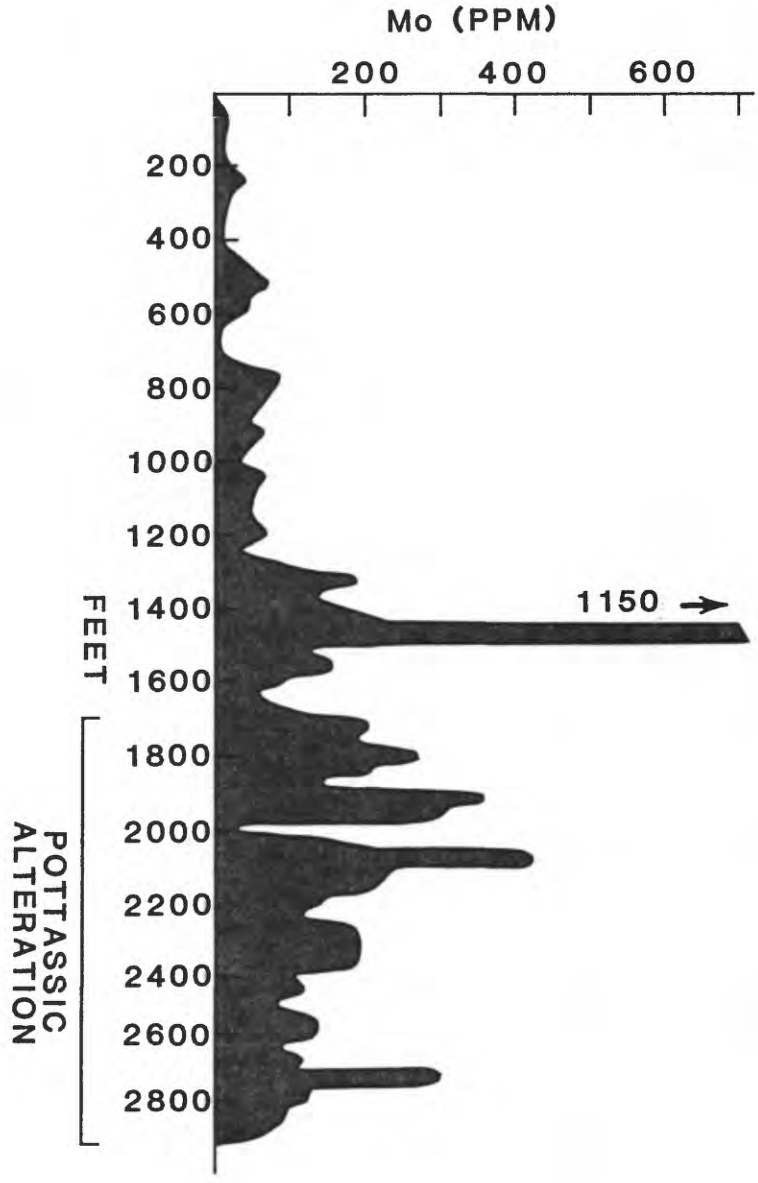
Mo (PPM)
200
400
600
200
400
600
800
1000
1200
1400
1600
1800
2000
2200
2400
2600
2800
FEET
1150
POTTASSIC ALTERATION

Figure 6a.

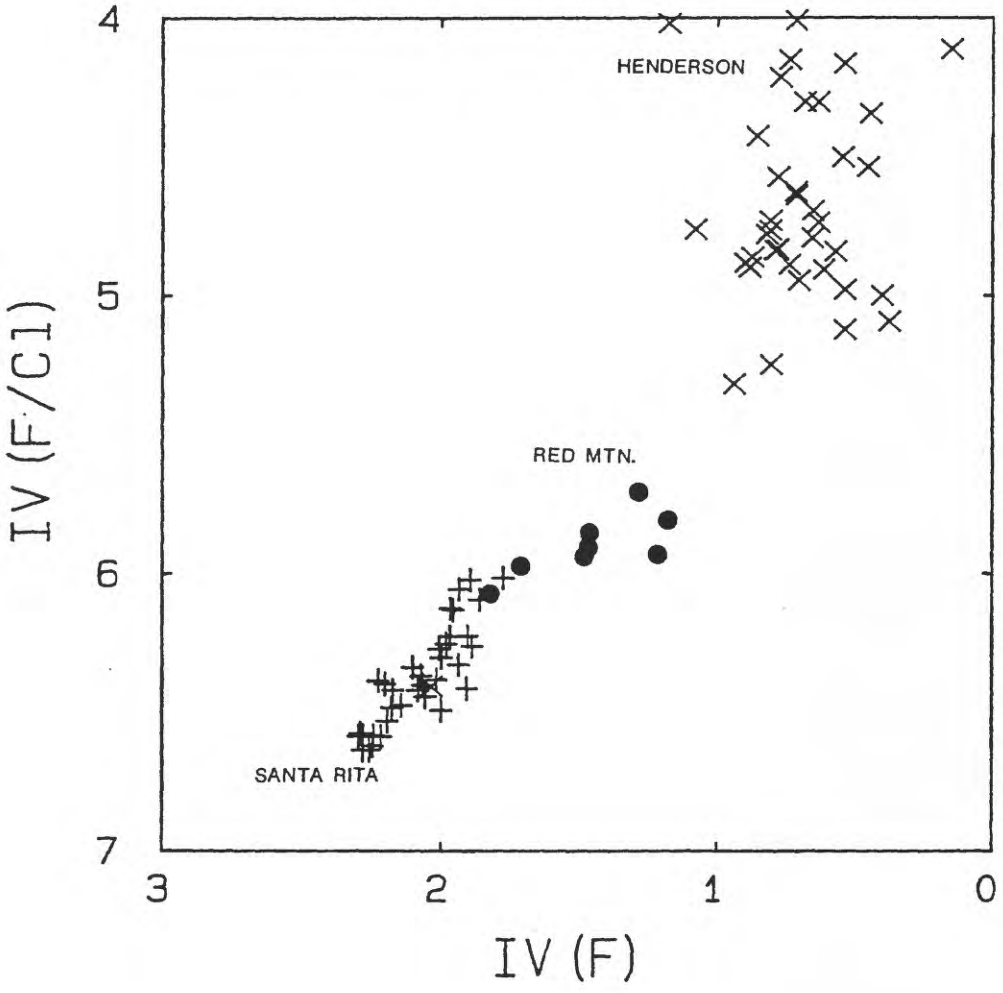

Figure 6b.

Figure 7a.

Figure 7b.

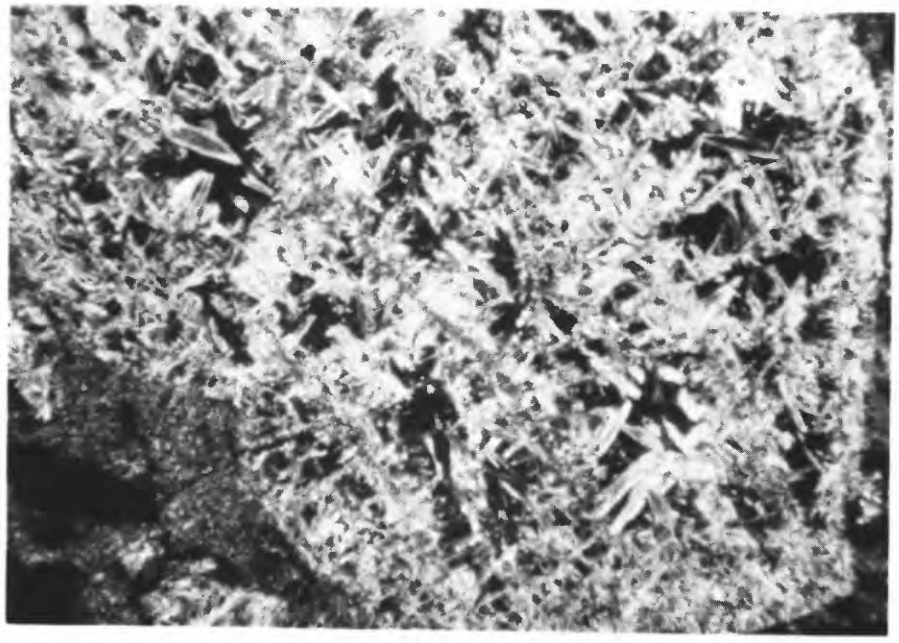

Figure 8a.

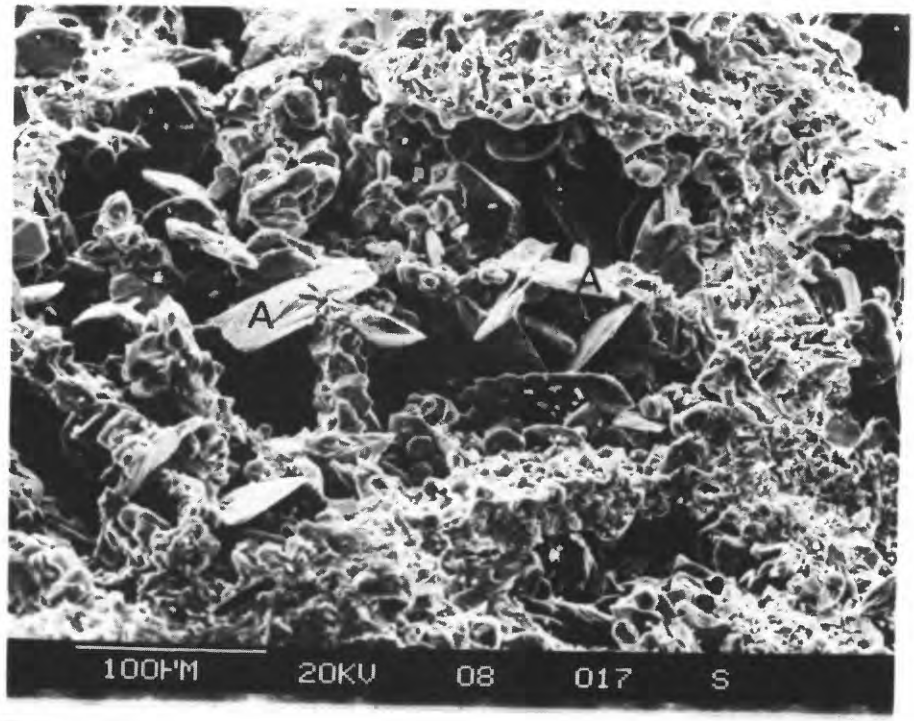

Figure 8b.

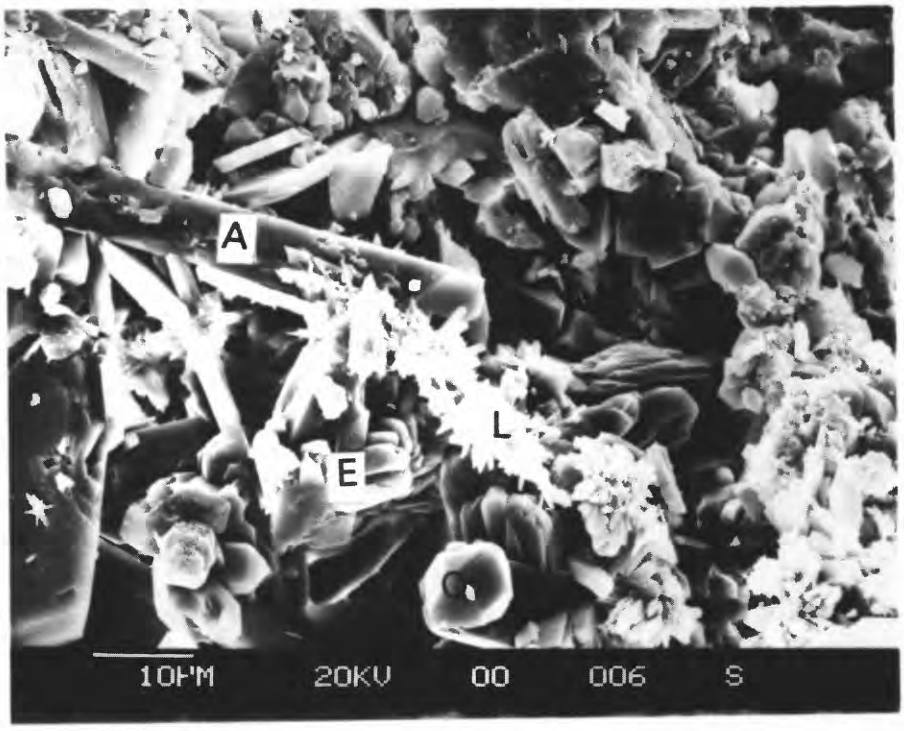

Figure 8c.

Figure 9.

Figure 10.

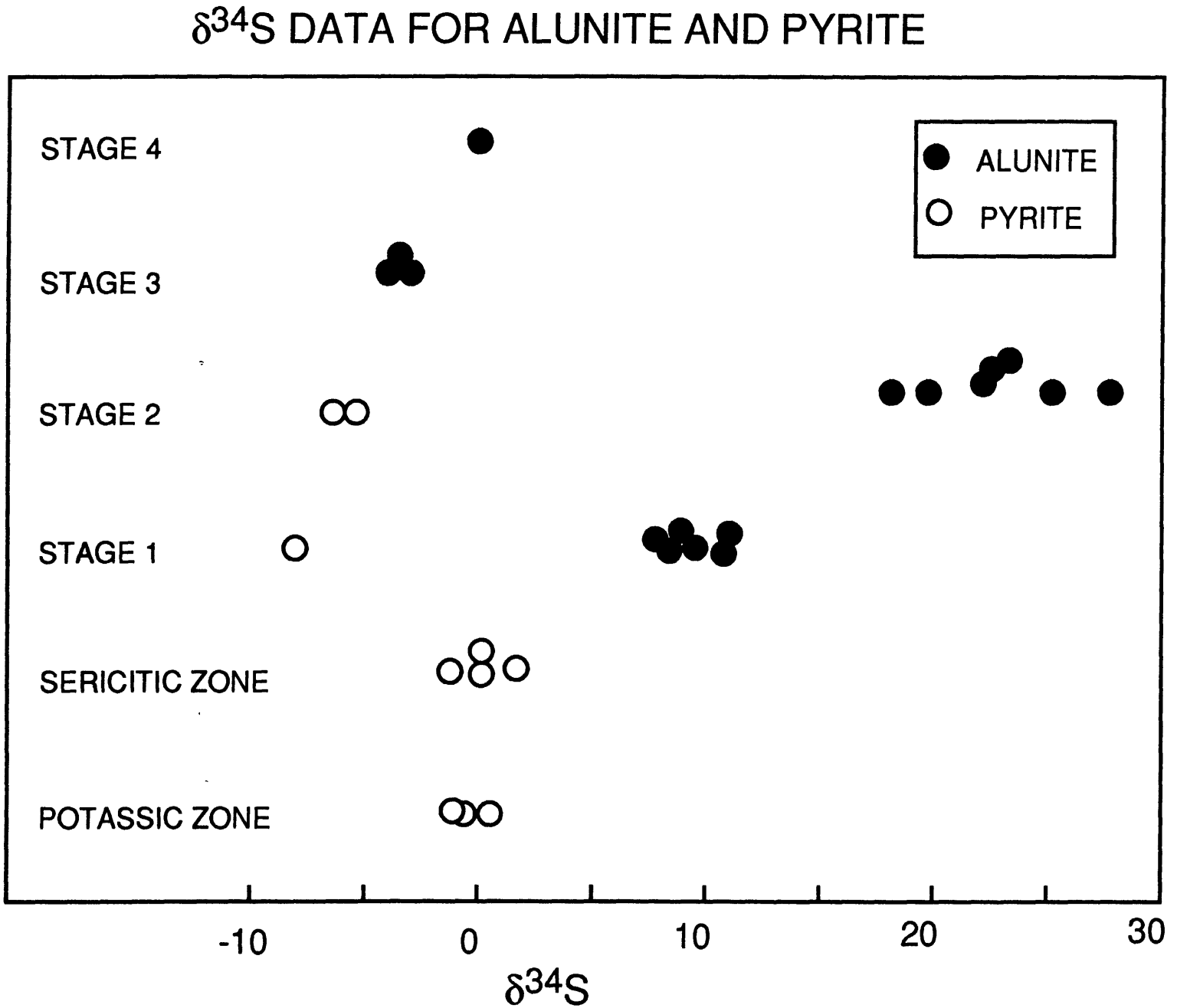
δ34S DATA FOR ALUNITE AND PYRITE
STAGE 4
STAGE 3
STAGE 2
STAGE 1
SERICITIC ZONE
POTASSIC ZONE
ALUNITE
PYRITE
-10
0
10
20
30
δ34S

Figure 11.

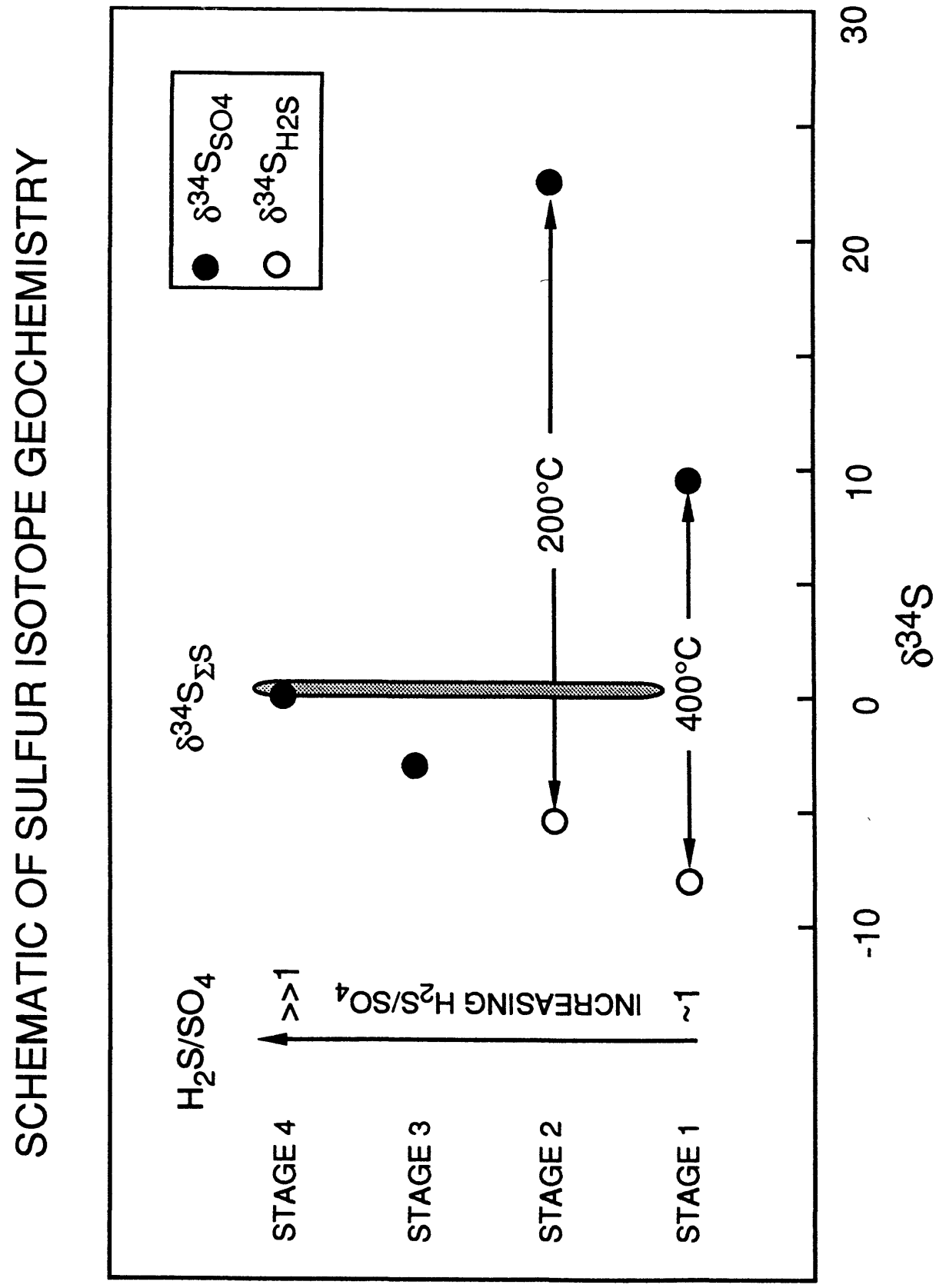
SCHEMATIC OF SULFUR ISOTOPE GEOCHEMISTRY
$\delta^{34}S_{SO4}$
$\delta^{34}S_{H2S}$
$\delta^{34}S_{\Sigma S}$
200°C
400°C
H_2S/SO_4
>>1
INCREASING H_2S/SO_4
~1
STAGE 4
STAGE 3
STAGE 2
STAGE 1
-10
0
10
20
30
$\delta^{34}S$

Figure 12.

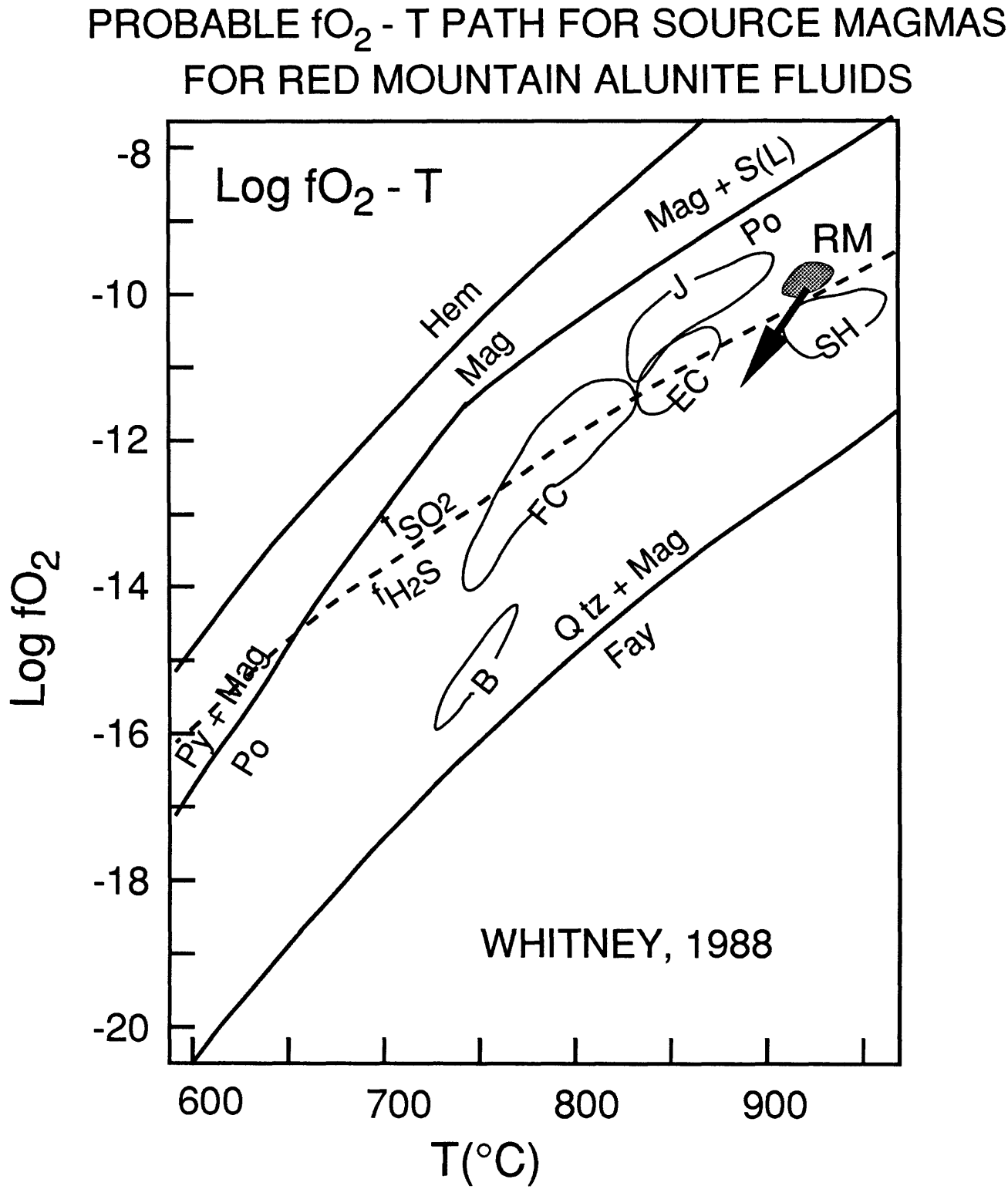
PROBABLE fO_2 - T PATH FOR SOURCE MAGMAS
FOR RED MOUNTAIN ALUNITE FLUIDS
Log fO_2 - T
Mag + S(L)
Po
RM
J
Hem
Mag
SH
EC
f_{SO_2}
FC
f_{H_2S}
Py + Mag
Po
B
Qtz + Mag
Fay
WHITNEY, 1988
-8
-10
-12
-14
-16
-18
-20
Log fO_2
600
700
800
900
T(°C)

Figure 13a.

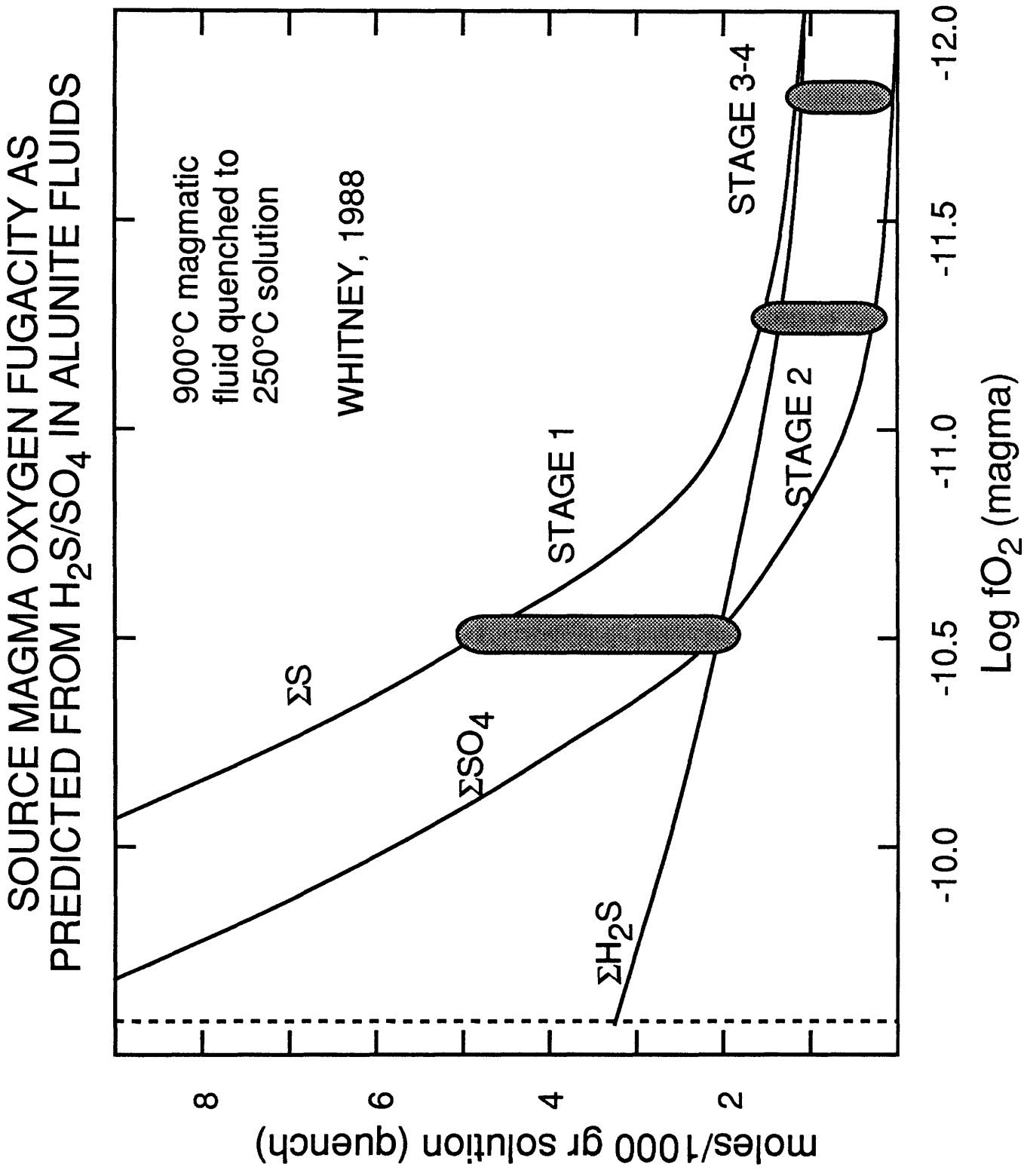
SOURCE MAGMA OXYGEN FUGACITY AS
PREDICTED FROM H_2S/SO_4 IN ALUNITE FLUIDS
900°C magmatic
fluid quenched to
250°C solution
WHITNEY, 1988
STAGE 3-4
STAGE 2
STAGE 1
ΣS
ΣSO_4
ΣH_2S
moles/1000 gr solution (quench)
8
6
4
2
-10.0
-10.5
-11.0
-11.5
-12.0
Log fO_2 (magma)

Figure 13b.

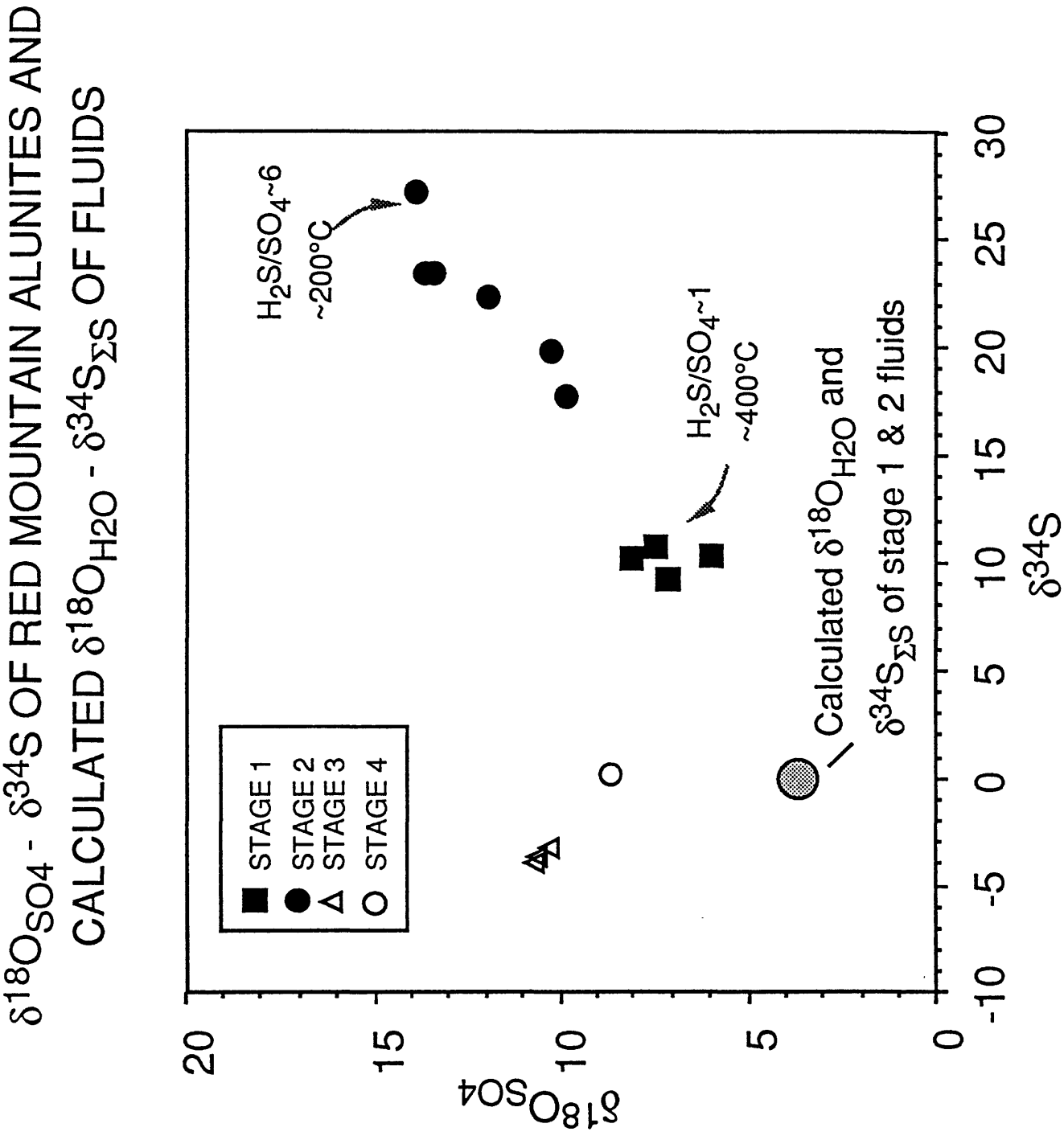
δ18OSO4 - δ34S OF RED MOUNTAIN ALUNITES AND
CALCULATED δ18OH2O - δ34SΣS OF FLUIDS
STAGE 1
STAGE 2
STAGE 3
STAGE 4
H2S/SO4~6
~200°C
H2S/SO4~1
~400°C
Calculated δ18OH2O and
δ34SΣS of stage 1 & 2 fluids
δ18OSO4
δ34S
20
15
10
5
0
-10
-5
0
5
10
15
20
25
30

Figure 14.

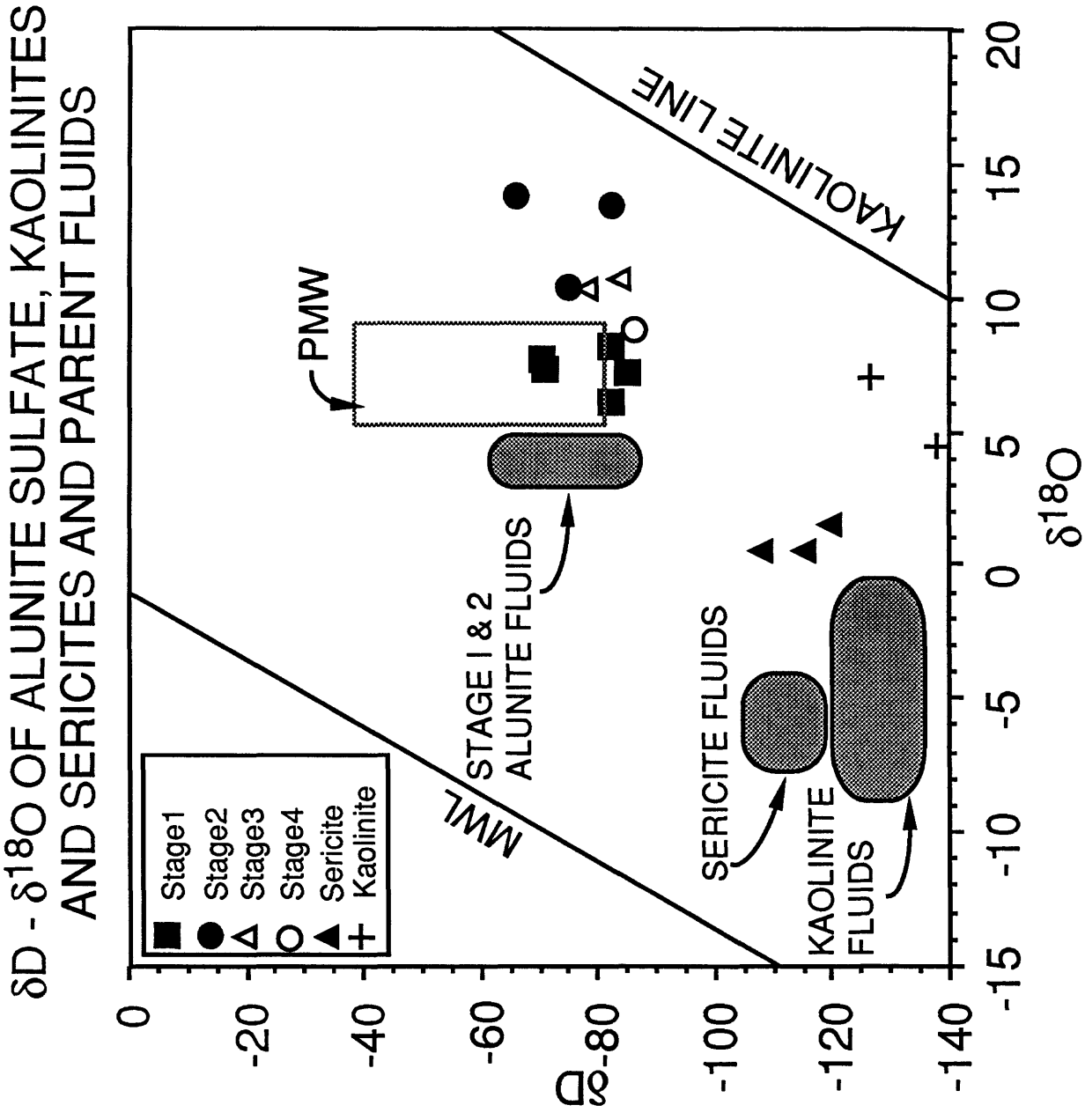
δD - δ18O OF ALUNITE SULFATE, KAOLINITES AND SERICITES AND PARENT FLUIDS
Stage1
Stage2
Stage3
Stage4
Sericite
Kaolinite
MWL
KAOLINITE LINE
PMW
STAGE I & 2 ALUNITE FLUIDS
SERICITE FLUIDS
KAOLINITE FLUIDS
δD
δ18O
0
-20
-40
-60
-80
-100
-120
-140
-15
-10
-5
0
5
10
15
20

Figure 15.

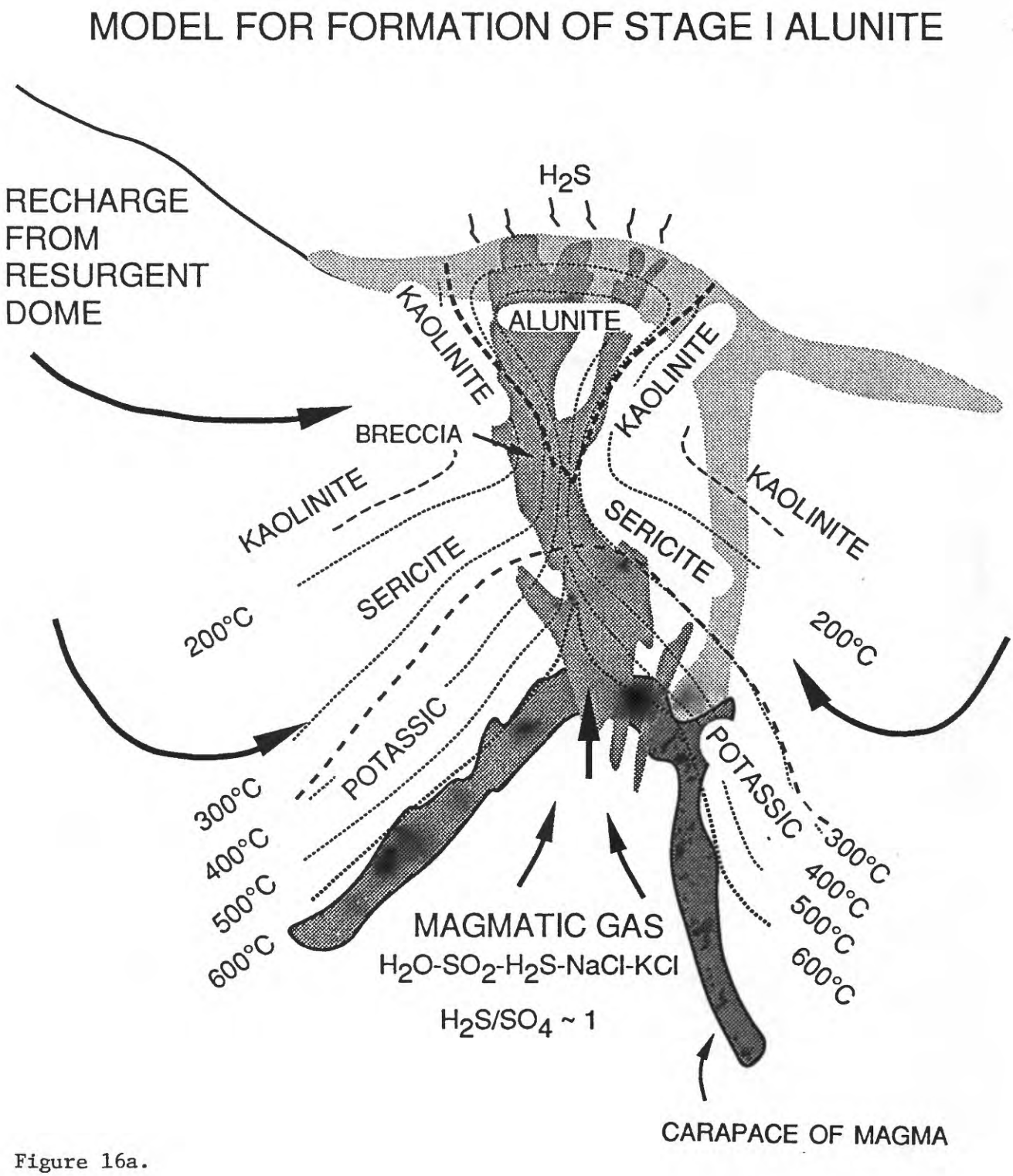
MODEL FOR FORMATION OF STAGE I ALUNITE
RECHARGE FROM RESURGENT DOME
H_2S
KAOLINITE
ALUNITE
KAOLINITE
BRECCIA
KAOLINITE
KAOLINITE
SERICITE
SERICITE
200°C
200°C
POTASSIC
POTASSIC
300°C
400°C
500°C
600°C
300°C
400°C
500°C
600°C
MAGMATIC GAS
H_2O-SO_2-H_2S-NaCl-KCl
H_2S/SO_4 ~ 1
CARAPACE OF MAGMA

Figure 16a.

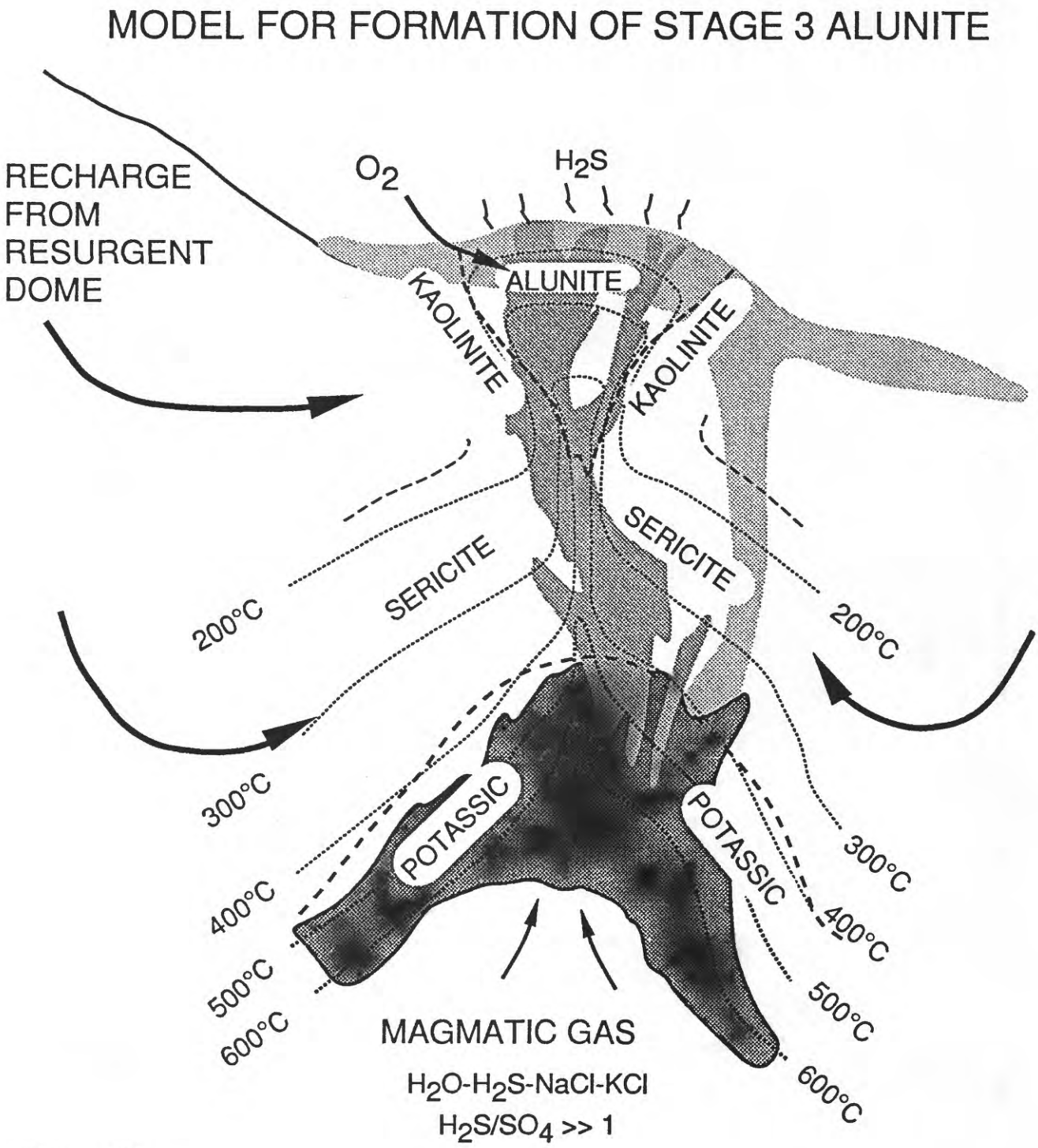
MODEL FOR FORMATION OF STAGE 3 ALUNITE
RECHARGE FROM RESURGENT DOME
O_2
H_2S
ALUNITE
KAOLINITE
KAOLINITE
SERICITE
SERICITE
200°C
200°C
300°C
300°C
400°C
400°C
500°C
500°C
600°C
600°C
POTASSIC
POTASSIC
MAGMATIC GAS
H_2O-H_2S-NaCl-KCl
H_2S/SO_4 >> 1

Figure 16b.